Metrological assessment of DC current comparator resistance bridges

# Metrological assessment of DC current comparator resistance bridges

Martina Marzano[a,*], Pier Paolo Capra[a], Cristina Cassiago[a], Vincenzo D'Elia[a], Enrico Gasparotto[a], Luca Callegaro[a]

[a] *Istituto Nazionale di Ricerca Metrologica (INRIM), Strada delle Cacce 91, Torino, 10135, Italy*

**Abstract**

Direct-current comparator bridges (DCC) are the working horses of primary resistance metrology in the intermediate resistance range. Having a ratio accuracy reaching $10^{-7}$ or better, they allow the realisation of resistance scales and the calibration of artifact standard resistors for customers. In this paper we compare the performances of three commercial DCC bridges, by performing measurements on resistors in decadal ratios (1 Ω to 10 kΩ) of very high stability in a thermostated environment. The results show that the three bridges give mutually compatible results within the manufacturer's specifications, therefore mutually validating the bridges; nevertheless, the readings time series show quite different statistical behavior, with internal correlations, making an evaluation of the Type A measurement uncertainty not trivial.

*Keywords:* Resistance measurement, Electrical instruments, Measurement units and standards
84.37.+q, 07.50.-e, 06.20.F

## 1. Introduction

Direct-current comparator bridges (DCC) [1] are instruments which can measure the resistance ratio between two four-terminal resistance standards $R_1$ and $R_2$ with a relative base accuracy of $1 \times 10^{-7}$ or better for the intermediate resistance range (1 Ω to 10 kΩ), and are therefore suitable for the realisation of a primary resistance scale and to sustain a calibration service in National Metrology Institutes and calibration laboratories. Commercial, fully-automated bridges are on the market since more than 40 years.

Research is ongoing at INRIM to simplify and automate the traceability chain for the maintained resistance standard and to perform calibration for customers, and commercial DCCs are employed as a check of the scaling in the intermediate resistance range, and as a direct calibration instrument for the low resistance scale (1 μΩ to 1 Ω). Verifying the measurement accuracy of the different DCCs employed is therefore a basic metrology verification requirement.

In this paper, we compare the performance of three different commercial DCCs in performing measurements on the maintained national standard of dc resistance, in the intermediate range.

## 2. Direct-current comparators

The direct-current comparator bridges (DCC) [2], whose simplified schematic is shown in Figure 1, measure resistance ratio between two four terminal-pair resistors $R_1$ and $R_2$. The resistors are energized by two current sources; the resulting currents $I_1$ and $I_2$ flow through two windings, having turns $N_1$ and $N_2$, wound on a ferromagnetic core. The magnetic flux in the

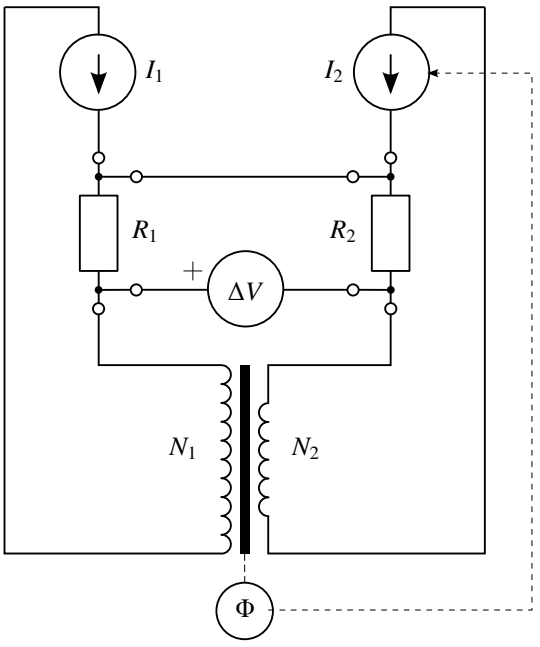


Figure 1: Simplified schematic diagram of a DCC bridge measuring resistors $R_1$ and $R_2$.

*m.marzano@inrim.it

| Nominal | 1 Ω | 10 Ω | 100 Ω | 1 kΩ | 10 kΩ |
|---|---|---|---|---|---|
| Type | Leeds & Northrup | Leeds & Northrup | ESI | ESI | ESI |
| Model | 4040-B | 4040-B | SR 105 | SR 105 | SR 104 |
| Thermostat | oil, 1 mK | oil, 1 mK | oil, 1 mK | oil, 1 mK | air, 5 mK |
| $\alpha$ | $4.1 \times 10^{-6}\,\mathrm{K}^{-1}$ | $2.4 \times 10^{-6}\,\mathrm{K}^{-1}$ | $4.0 \times 10^{-9}\,\mathrm{K}^{-1}$ | $2.3 \times 10^{-7}\,\mathrm{K}^{-1}$ | $5.4 \times 10^{-8}\,\mathrm{K}^{-1}$ |
| $\beta$ | $-5.0 \times 10^{-7}\,\mathrm{K}^{-2}$ | $-5.4 \times 10^{-7}\,\mathrm{K}^{-2}$ | $-2.5 \times 10^{-8}\,\mathrm{K}^{-2}$ | $3.0 \times 10^{-9}\,\mathrm{K}^{-2}$ | $-3.3 \times 10^{-8}\,\mathrm{K}^{-2}$ |
| One year stability | $0.088 \times 10^{-6}$ | $-0.19 \times 10^{-6}$ | $0.012 \times 10^{-6}$ | $0.24 \times 10^{-6}$ | $0.026 \times 10^{-6}$ |

Table 1: The resistors employed in the comparison. $\alpha$ and $\beta$ are the temperature coefficients near the operating temperature.

core is given by $\mathcal{R}\Phi = N_1 I_1 - N_2 I_2$, where $\mathcal{R}$ is the reluctance of the core. $\Phi$ is measured by a fluxgate detector [1, 3, 4], whose output constitutes the error signal of a feedback control. The output of such control drives one of the two current sources (e.g., $I_2$) to keep $\Phi = 0$ and therefore the condition $N_1 I_1 = N_2 I_2$. The voltage difference $\Delta V = R_1 I_1 - R_2 I_2$ between the two resistors is measured, and the turns of one of the two windings (say, $N_2$) are also adjusted to set $\Delta V$ to a minimum. This second adjustment was manual in early bridges [1] and is presently also automated [5]. The readings of the bridge are the two values $N_1/N_2$ and $\Delta V$, which give the measurement equation

$$\frac{R_1}{R_2} = \frac{N_1}{N_2}\left(1 - \frac{\Delta V}{R_2 I_2}\right). \tag{1}$$

During the measurement the currents $I_1$ and $I_2$ are periodically reversed to reduce the influence of voltage offsets.

The DCC bridge measurement accuracy [6] is limited by the sensitivities of the flux detector and of the voltage detector which sense $\Delta V$, and by flux leakages in the magnetic circuit. Bridges measuring resistors in the μΩ to the MΩ range are available; best accuracy is achieved for medium-ranged resistors (1 Ω to 10 kΩ) and ratios within the 10 : 1 range.

The DCCs under comparison are three different models from the Measurement International that acquired at different times. In the following, the measurements are labelled as follows:

**6010B** Measurement International model 6010B, serial 1020904, acquired in 2006.

**6010D** Measurement International model 6010D, serial 1104668, acquired in 2021.

**6010Q** Measurement International model 6010Q, serial 1100670, acquired in 2008.

## 3. Measurement procedure

The comparison of the three bridges required equipment consisting of a series of high stability standard resistors, a Guildline VT9732 oil bath, a Kambic TK-105 US air bath and a low noise switching system. Table 1 reports the resistors employed in the comparison, which have nominal values in the 1 Ω to 10 kΩ range, and their main characteristics. The bridges and the resistors are connected by means of an automatic Leeds & Northrup type rotary switch system with low thermo-electromotive forces (less than 5 nV). The comparison of the bridges, whose measurements could not be made at the same time, was possible due to the high stability of the standards used both in short and medium term (less than $2 \times 10^{-7}$ per year), and of the influence parameters.

| Ratio | $I_1$/ mA | $t_{\mathrm{set}}$/s | *Filter* | 6010Q #*ADC* |
|---|---|---|---|---|
| 10/1 | 10 | 6 | 3 | 6 |
| 100/10 | 3 | 8 | 3 | 8 |
| 1k/100 | 1 | 8 | 3 | 8 |
| 10k/1k | 0.1 | 12 | 3 | 12 |

Table 2: Measurements settings employed in the measurements of the 10/1, 100/10, 1k/100 and 10k/1k ratios with the 6010B, 6010D and 6010Q DCC bridges.

We label the ratio measurements between 10 Ω and 1 Ω, 100 Ω and 10 Ω, 1 kΩ and 100 Ω, 10 kΩ and 1 kΩ as 10/1, 100/10, 1k/100 and 10k/1k, respectively. All the ratios were measured with the 6010B, 6010D and 6010Q DCC bridges in sequence by employing the same resistance standards and the same measurement configurations, reported in Table 2. For all the bridges it is possible to set the desired current $I_1$ for the highest resistor under test $R_1$, the settle time $t_{\mathrm{set}}$ between the current reversal during the measurement and the filter size *Filter* corresponding to the number of averaged values (*Filter* × 10, where *Filter* can assume the values 0.3, 1 or 3) before each value is displayed. For only the 6010Q DCC bridge, it is possible to set the parameter #*ADC* representing the number of conversions of the analog-to-digital converters. For the 6010B and 6010D bridges, each reading lasts for a time equal to the chosen $t_{\mathrm{set}}$. For the 6010Q, the acquisition time of each reading is longer (about twice the chosen $t_{\mathrm{set}}$) because of the #*ADC* parameter.

The three bridges were automatically controlled by the same software developed specifically for the comparison that ensures the same procedure and execution of the measurements with similar integration times.

## 4. Uncertainty

### 4.1. Type A components

The expression of the type A uncertainty is nontrivial, since each time series of the readings performed by the bridges display internal correlations, and therefore the standard deviation of the mean underestimates the real uncertainty. Figures 2, 3 and 4 show examples of a measurement acquisition of the

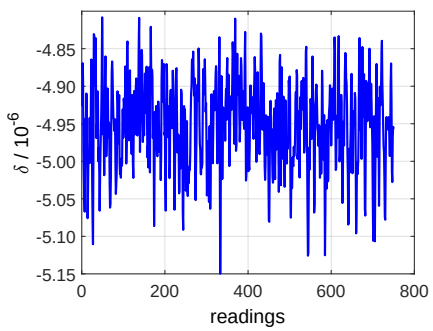


Figure 2: Example of a measurement acquisition of the 10k/1k ratio with the 6010B DCC bridge. The total acquisition time is about 3 h.

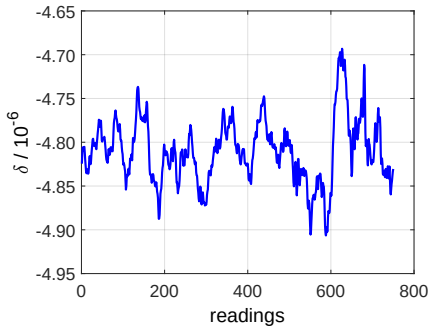


Figure 3: Example of a measurement acquisition of the 10k/1k ratio with the 6010D DCC bridge. The total acquisition time is about 3 h.

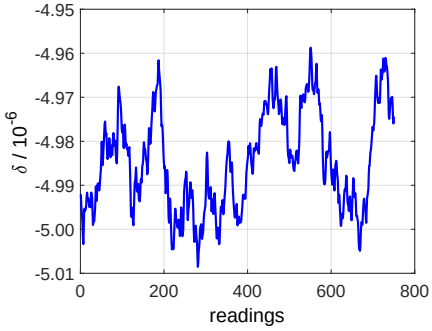


Figure 4: Example of a measurement acquisition of the 10k/1k ratio with the 6010Q DCC bridge. The total acquisition time is about 5 h.

10k/1k ratio performed with the 6010B, 6010D and 6010Q bridges, respectively, in the same measurements conditions. For clarity, we plot the relative deviation $\delta$ of the measured ratios from the nominal value 10.

As stated by the *Guide to the expression of uncertainty in measurement* [7, 4.2.7], if the random variations of the observations of an input quantity are correlated in time, the experimental standard deviation of the mean may be inappropriate estimator of the type A uncertainty. Better estimates can be determined by considering the Allan deviation [8]. We follow an approach proposed by N. F. Zhang of the National Institute for Standards and Technology [8, 9, 10] very recently (2022) consolidated as an ISO standard [11].

The approach considers the sample autocorrelation function $\rho(i)$, calculated from the readings $x_k$ (where $i, k = 1 \ldots N$). The function gives the degree of correlation between two readings separated by a lag $i$. If $\rho(i) = 1$, the readings are totally correlated (that is, they are in fact the same reading, duplicated at lag $i$); if $\rho(i) = 0$, then the readings at lag $i$ are totally uncorrelated. In general, for readings processed through an analog or digital low-pass filter, $\rho(i)$ decreases with increasing lag $i$.

The type A uncertainty of the measurement is calculated as the standard deviation of the mean multiplied by an expansion factor $m \geq 1$, computed from $\rho(i)$ as follows:

$$m = \left[ 1 + \frac{2}{N} \sum_{i=1}^{N_r - 1} (N - i)\rho(i) \right]^{1/2} , \qquad (2)$$

where $N_r \leq N$ is evaluated by considering only $\rho(i)$ above a significance threshold. Uncorrelated readings give $m = 1$, and the type A uncertainty is the standard deviation of the mean. Autocorrelated readings give $m > 1$ and hence a type A uncertainty larger than the standard deviation of the mean. This is understandable if one considers that, if two readings are correlated, the information provided by the couple is partly redundant.

Figure 5 shows an example of the calculation outcome.

The three bridges show significant differences in the correlation span and magnitude of the readings time series, and the calculation of $m$ gives different results. For the measurements performed, these range from $m = 1.5 \ldots 2.1$ for the MI6010B, $m = 4.8 \ldots 5.1$ for the MI6010D, $m = 5.1 \ldots 8.1$ for the MI6010Q.

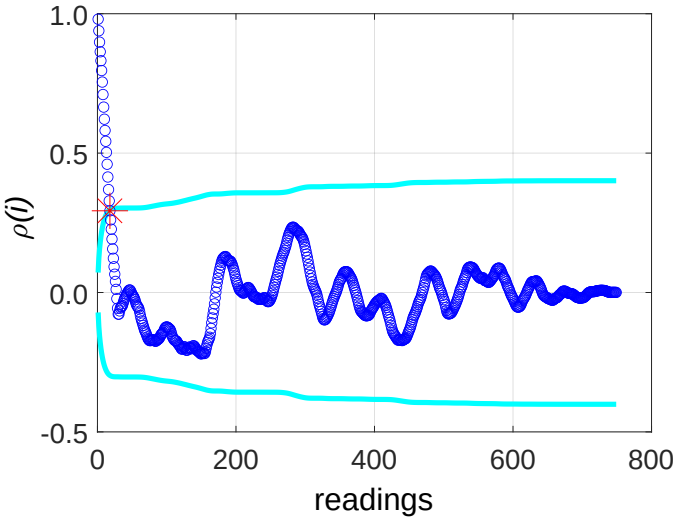


Figure 5: Example of the outcome of the calculation of the sample correlation $\rho(i)$ of the readings, corresponding to the measurement acquisition of the 10k/1k ratio with the 6010D DCC bridge reported in Figure 3. The light blue lines are a significance threshold; a correlation span of 18 points is considered in Equation 2.

### *4.2. Type B components to the uncertainty*

The type B uncertainty components considered are the following:

- Thermal stability of the standard resistors involved in the comparison. The contribution to the uncertainty is evaluated as the maximum absolute deviation of the resistor value due to a temperature (positive or negative) span corresponding to the specified stability of the thermal bath.

- Time stability of the resistors. The standards are monitored and the corresponding drifts known over a period of years. The contribution to the uncertainty is evaluated by considering an uncorrected time drift over the measurement period.

- Electrical isolation. The uncertainty contribution is evaluated as the maximum deviation caused by a 1 TΩ parasitic resistor in parallel with the largest resistor involved in the comparison.

| $R_1$ | $R_2$ | Thermal stability | Time drifts | Isolation | Type A | $u(R_1/R_2)$ |
|---|---|---|---|---|---|---|
| 10 kΩ | 1 kΩ | $3.6 \times 10^{-10}$ | $3.3 \times 10^{-9}$ | $1.0 \times 10^{-8}$ | $3.2 \times 10^{-9}$ | $2.2 \times 10^{-8}$ |
| 1 kΩ | 100 Ω | $2.3 \times 10^{-10}$ | $3.3 \times 10^{-9}$ | $1.0 \times 10^{-9}$ | $4.3 \times 10^{-10}$ | $7.0 \times 10^{-9}$ |
| 100 Ω | 10 Ω | $2.4 \times 10^{-9}$ | $2.6 \times 10^{-9}$ | $1.0 \times 10^{-10}$ | $2.9 \times 10^{-10}$ | $7.1 \times 10^{-9}$ |
| 10 Ω | 1 Ω | $4.8 \times 10^{-9}$ | $2.9 \times 10^{-9}$ | $1.0 \times 10^{-11}$ | $5.8 \times 10^{-10}$ | $1.1 \times 10^{-8}$ |

Table 3: Uncertainty budget for comparisons performed with the MI6010B bridge.

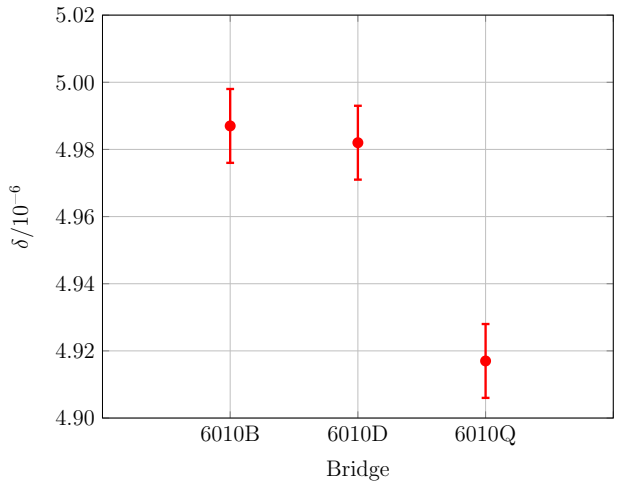


Figure 6: **10/1 ratio**. $\delta$ is the relative deviations from the nominal ratio 10/1 for different measurements performed in about 5 days with the 6010B, 6010D and 6010Q bridges. The uncertainty bars report the expanded uncertainty ($k = 2$) of each measurement.

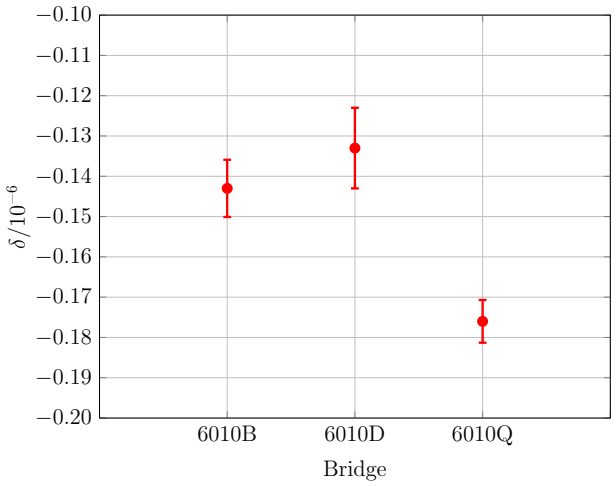


Figure 7: **100/10 ratio**. $\delta$ is the relative deviations from the nominal ratio 100/10 for different measurements performed in about 5 days with the 6010B, 6010D and 6010Q bridges. The uncertainty bars report the expanded uncertainty ($k = 2$) of each measurement.

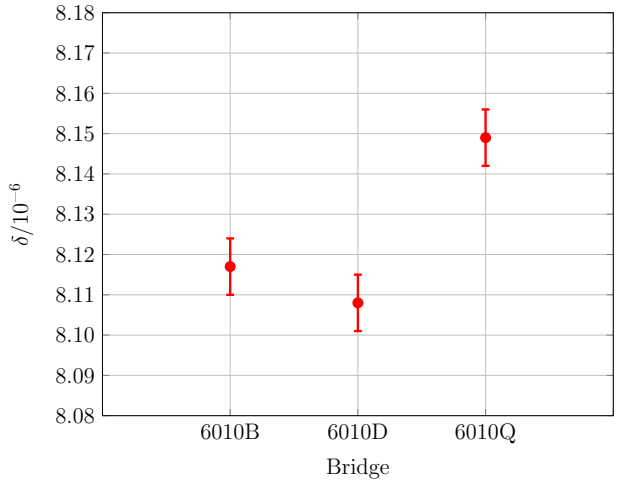


Figure 8: **1k/100 ratio**. $\delta$ is the relative deviations from the nominal ratio 1k/100 for different measurements performed in about 5 days with the 6010B, 6010D and 6010Q bridges. The uncertainty bars report the expanded uncertainty ($k = 2$) of each measurement.

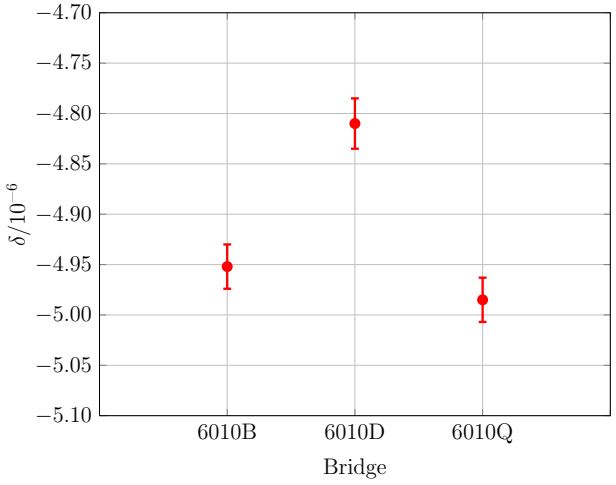


Figure 9: **10k/1k ratio**. $\delta$ is the relative deviation from the nominal ratio 10k/1k for different measurements performed in about 5 days with the 6010B, 6010D and 6010Q bridges. The uncertainty bars report the expanded uncertainty ($k = 2$) of each measurement.

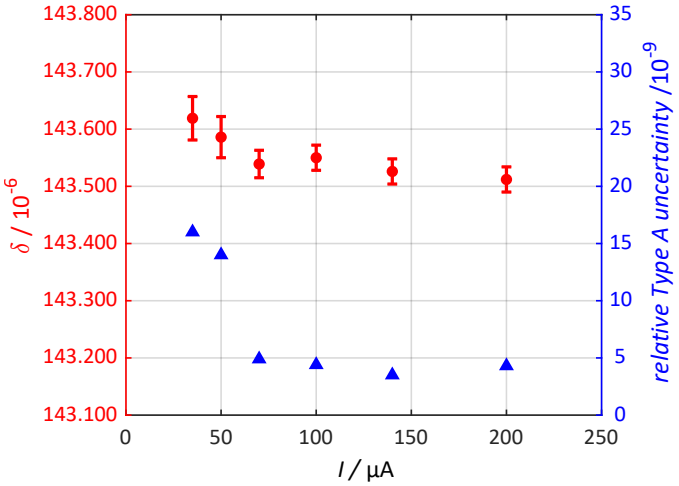


Figure 10: Current dependence of the 10k/1k ratio measurements performed with the 6010D bridge. Red marks are the $\delta$ for different values of current applied to the 10 kΩ resistance standard and the error bars report the expanded relative uncertainties of the measurements ($k = 2$). Blue marks are the relative type A uncertainties of the measurements, calculated as in Section 4.1.

The uncertainty budget for the ratio measurements performed with the MI6010B is given in Table 3. The budgets for the 6010D an 6010Q have the same structure.

## 5. Results

Figures 6, 7, 8 and 9 show the comparison among the results obtained with the 6010B, 6010D and 6010Q DCC bridges in the measurements of the 10/1, 100/1, 1k/100 and 10k/1k, respectively. Each plot reports the relative deviation $\delta$ of the measured ratio from the nominal ratio obtained from several measurements performed in about 5 days. In all figures the results are obtained from 800 repeated measurements. The corresponding acquisition time is dependent on the chosen $t_{set}$, reported in Table 2 for each measured ratio, and ranges from about 2 h for the 10/1 ratio to about 4 h for the 10k/1k ratio.

Figure 10 shows the current dependence of the 10k/1k ratio measurements performed with the 6010D bridge. For these measurements, different resistance standards were employed: a custom-made 1 kΩ resistor made from the parallel of 10 Vishay VHA 512T 10 kΩ components (tolerance ±0.005%) thermostated at about 27 °C; a Tinsley 5685A 10 kΩ resistance standard, with a nominal stability of 0.5 ppm/year, thermostated in a Kambic TK-109 US air bath. The plot reports in red the dependence of $\delta$ with the error bars given by expanded relative uncertainties; in blue, the type A uncertainties of the measurements. The reported currents are those applied to the 10 kΩ resistance standard.

## 6. Discussion

Even though the three bridges come from the same manufacturer and are realised with similar technologies, the three time series of Figures 2, 3 and 4 have a different behaviour and show a different amount of internal correlations. This might be due to different raw data processing performed by the bridge firmwares. The Type A contributions to the measurement uncertainty are therefore computed accordingly to a recently published ISO standard [11].

The short-term stability of the resistors due to drift and temperature variations can be estimated to be better than $3 \times 10^{-10}$ over a day, hence the deviations between the readings of the three bridges are related only to the reading noise and the bridge ratio errors.

In Figures 6, 7, 8 and 9, where the error bars represent the expanded uncertainties of the measurements, the results appear not compatible. The reported differences between the different estimates, however, are smaller than the manufacturer specifications of the relative errors of the bridges (of several parts in $10^8$ for each bridge). The measurements, therefore, provide a mutual validation of the three bridges.

The bridge ratio errors can be determined in an absolute way by comparing their readings with those of a cyrogenic current comparator [12], which allows measurements accuracies of parts in $10^9$ and thus in this sense can be considered a perfect reference. A comparison experiment is under planning.

Figure 10 shows that increasing the measurement current the bridge precision increases. Considering the scheme of Figure 1, this is compatible with both (a) the increase of the magnetic field generated by the windings and thus a better sensitivity of the flux detector and (b) the increase of $\Delta V$ for a given deviation from equilibrium, and thus of an increase of the relative accuracy of the correction term in the bridge equilibrium Equation 1. Figure 10 shows also an evolution of the measurement value. The origin of this second phenomenon can be related to several causes, including residual hysteretical effects in the ferromagnetic core of the comparator or threshold effects in the managing bridge firmware, difficult to investigate with a black box approach applied to a commercial instrument.

## 7. Acknowledgements

This work is supported by the project MIUR PRIN 2020A2M33J CAPSTAN Quantum electrical Italian national capacitance standard.

## References

[1] M. P. MacMartin, N. L. Kusters, A direct-current-comparator ratio bridge for four-terminal resistance measurements, IEEE Trans. Instr. Meas. 15 (4) (1966) 212–220.

[2] W. J. M. Moore, P. N. Miljanic, The current comparator, Vol. 4 of IEE electrical measurement series, Peter Peregrinus Ltd, London, UK, 1988, iSBN 0863411126.

[3] P. Odier, DCCT technology review, in: A. Peters, H. Schmickler, K. Wittenburg (Eds.), Proc. of Workshop on DC current transformers and beam-lifetime evaluations, CARE-HHH-ABI Networking, Lyon, France, 2004, pp. 3–5, 1–2 Dec 2004.

[4] P. Ripka, Electric current sensors: a review, Meas. Sci. Technol. 21 (2010) 112001, 23 pp.

[5] D. Brown, A. Wachowicz, S. Huang, The enhanced performance of the DCC current comparator using AccuBridge technology, in: 2016 Conference on Precision Electromagnetic Measurements (CPEM 2016), Ottawa, ON, Canada, 2016, pp. 1–2, 10–15 July 2016.

[6] S. Haiming, The uncertainty evaluation of automatic direct current comparator bridge, in: Conference Digest Conference on Precision Electromagnetic Measurements, Ottawa, Ontario, Canada, 2002, pp. 58–59, 16-21 June, 2002.

[7] Joint Committee for Guides in Metrology JCGM, 100:2008 (GUM 1995 with minor corrections) "Evaluation of measurement data — Guide to the expression of uncertainty in measurement" (2008).
URL www.bipm.org

[8] T. J. Witt, Practical methods for treating serial correlations in experimental observations, Eur. Phys. J.: Spec. Top. 172 137–152.

[9] N. F. Zhang, Calculation of the uncertainty of the mean of autocorrelated measurements, Metrologia 43 (4) (2006) S276–S281.

[10] A. F. Rigosi, A. R. Panna, S. U. Payagala, M. Kruskopf, M. E. Kraft, G. R. Jones, B.-Y. Wu, H.-Y. Lee, Y. Yang, J. Hu, D. G. Jarrett, D. B. Newell, R. E. Elmquist, Graphene devices for tabletop and high-current quantized Hall resistance standards, IEEE Trans. Instr. Meas. 68 (6) (2019) 1870–1878.

[11] ISO, 24185:2022 Evaluation of the uncertainty of measurements from a stationary autocorrelated process (Aug. 2022).
URL www.iso.ch

[12] J. Williams, Cryogenic current comparators and their application to electrical metrology, IET Science, Measurement & Technology 5 (2011) 211–224.